Journal of Wind Engineering & Industrial Aerodynamics 173 (2018) 156–170

Contents lists available at ScienceDirect

Journal of Wind Engineering & Industrial Aerodynamics

journal homepage: www.elsevier.com/locate/jweia

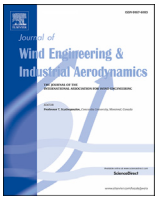

Aerodynamic behavior of a cable-stayed bridge section composed by inclined parallel decks

G.J.Z. Núñez [a], [*], A.M. Loredo-Souza [b], M.M. Rocha [b], F. Bagatini-Cachuço [b]

[a] Department of Design and Graphics, Faculty of Architecture, Universidade Federal do Rio Grande do Sul, Rua Sarmento Leite, 320 Porto Alegre, Brazil
[b] Department of Civil Eng., Faculty of Engineering, Universidade Federal do Rio Grande do Sul, Av. Osvaldo Aranha, 99 Porto Alegre, Brazil

ARTICLE INFO

Keywords:
Parallel bridges
Interference
Wind tunnel
Bridge aerodynamics
Vortex-shedding

ABSTRACT

The understanding of bridge aerodynamic behavior for specific cases with more than one deck is of great importance for structural design. The resultant interference effects caused by one or more windward decks are difficult to predict as they may reduce or increase resultant forces and displacements in leeward decks. This paper presents an experimental study on the transversal response to wind loads of a bridge sectional model with parallel decks. Wind tunnel tests were performed to identify static and dynamic behaviours for different interference scenarios and other additional tests were performed with single deck cases. Results indicated protection when decks were horizontally aligned and amplification as well as reduction of aerodynamic coefficients for decks in different vertical positions. Finally, a conclusive discussion is presented identifying possible reasons for the increases and reductions observed in interference cases.

1. Introduction

Long-span bridges are wind sensitive structures commonly used to solve traffic demand issues. Frequently, bridges are constructed in parallel to existent ones, while other new bridges are designed with two or more parallel decks. Usually, long-span cable stayed and suspension bridges are slender and flexible structures. Therefore, specific cases of parallel decks may develop relevant aerodynamic effects.

Previous studies discussed aerodynamic coefficients for different bridge deck shapes (Ostenfeld and Larsen, 1992; Miyata and Yamaguchi, 1993) as other researchers analyzed wind-structure interaction (Scanlan and Tomoko, 1971; Tanaka and Davenport, 1982; Ito and Nakamura, 1982; Irwin et al., 1997). However, wind effects are not fully understood for single deck bridges and, when two or more decks are built in parallel, complicated interference effects may occur, thus resulting in different responses when compared to the single deck case (Honda et al., 1990, 1993). Interference effects on bridge decks may be distinguished as (i) static aerodynamic interference and (ii) dynamic interference.

Interference effects generated by parallel decks are sensitive to vertical and horizontal distances between decks. In earlier studies, researchers exposed relevant alterations in lift and torque coefficients for horizontal distances between decks lower than 1.2B (Liu et al., 2009), where B is the alongwind cross-sectional dimension, as seen in Fig. 1(d). Other previous investigations for cases with different deck shapes and a horizontal offset slightly smaller than the dimension B resulted in reduction on drag coefficients as well as increases on lift coefficients for the leeward section (Larsen et al., 2000). Studies conducted with Tacoma Narrows parallel decks identified minor changes on lift and torque for horizontal distances up to 3.39B, considering the smaller deck width (Irwin et al., 2005). Other later studies on parallel box girders resulted in interference effects for distances in a range of 8B (Kimura et al., 2008). Thus, a dependency between decks separation distance and magnitude of interference effects is noticed as the leeward deck is often situated within the windward deck wake region.

Recent findings reveal that dynamic interference effects for parallel decks are even more complex. Reduction and/or amplification of responses can occur depending on the particularities of each case. Studies based on both in-situ measurements (Kim et al., 2013) and wind tunnel tests (Kimura et al., 2008) identified a phenomenon where the leeward deck motion was significantly affected by windward deck motion. These findings proved that when the windward deck is not oscillating, the leeward deck can develop an intense sinusoidal response. In terms of vortex-induced vibration (VIV) response, interference effects were proven to be sensitive to gap width as well as the decks shape (Meng et al., 2011). Other findings led to interference effects affecting the windward section VIV response (Seo et al., 2013). Moreover, recent

---

[*] Corresponding author.
E-mail addresses: gustavo.javier@ufrgs.br (G.J.Z. Núñez), acir@ufrgs.br (A.M. Loredo-Souza), mmrocha@ufrgs.br (M.M. Rocha), bagatini.cachuco@ufrgs.br (F. Bagatini-Cachuço).

https://doi.org/10.1016/j.jweia.2017.12.015
Received 30 October 2016; Received in revised form 10 December 2017; Accepted 10 December 2017

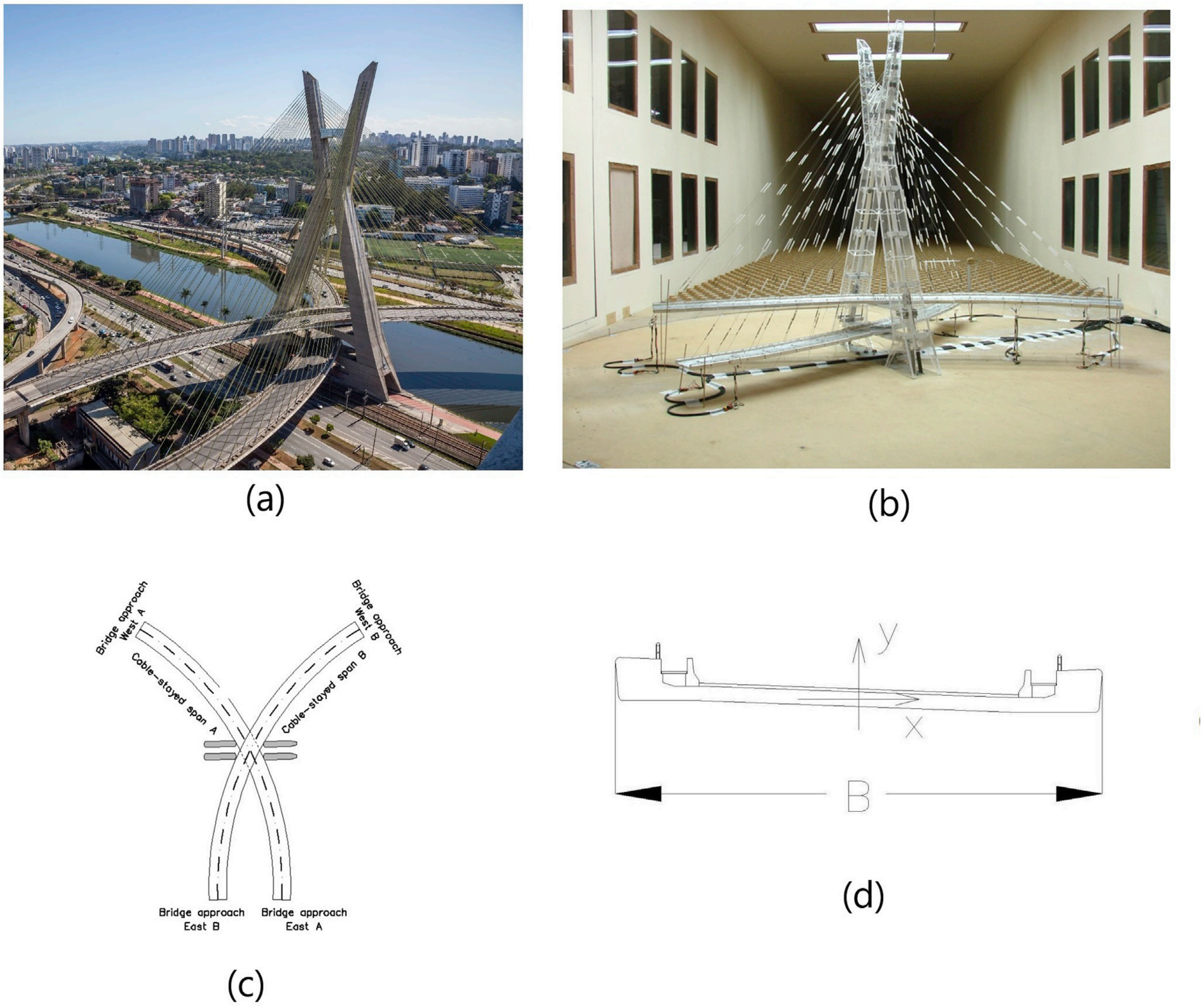

Fig. 1. *Octavio Frias de Oliveira* Bridge in Sao Paulo, Brazil: (a) full-scale structure, (b) full aeroelastic model, (c) plant view, and (d) cross-section reference dimension B.

studies indicate that flutter instability tends to diminish as the gap width increases while VIV response is also affected (Kargarmoakhar et al., 2015).

In this study, wind tunnel tests were performed with two parallel deck sections for different interference configurations. The adopted deck sections are a reduced scale model of *Octavio Frias de Oliveira* Cable-Stayed Bridge deck sections shown in Fig. 1. Varied horizontal and vertical gaps were tested as well as additional single deck cases. The aerodynamic behavior was analyzed in terms of aerodynamic coefficients, pressure distributions and dynamic response. Moreover, additional hot-wire anemometry was performed to identify flow characteristics inside the wake region. Both reduction and amplification were observed due to interference.

Although this paper presents the results derived from sectional (2D) models, the real bridge design included the investigation performed in a full aeroelastic (3D) model, as shown in Fig. 1(b). However, the results from the latter are not included in this paper.

2. Full-scale and sectional model properties

Wind tunnel simulations were performed with a reduced scale model of *Octavio Frias de Oliveira* Cable-Stayed Bridge deck section. The full-scale structure is composed by two decks and has a central cable-stayed span of 290 m length supported by a single tower with 138 m high, as shown in Fig. 1. Both of its decks have a 10.51 m width roadway and 16 m of total width, presented in Fig. 2 (a), while the wind tunnel model geometric scale is 1:50 as shown in Fig. 2 (b) in millimeters. Each deck superelevation of 3.7% is orientated according to the respective course curvature.

Full-scale structure dynamic parameters were estimated with numerical modeling in design phases and are presented in Table 1 together with the corresponding parameters for the sectional model. The ratio of 2.67 for torsional/vertical natural frequencies was maintained for the sectional model through calibration of polar moment of inertia and stiffness. Since full-scale measurements were not performed, two levels of structural damping were considered for the sectional model: 0.10% and 0.22% for vertical vibrations and 0.10% and 1.30% for torsion.

3. Wind tunnel flow characteristics

Reduced scale simulations were performed in a test chamber with a cross section of 1.30 m × 0.90 m at *Professor Joaquim Blessmann* wind tunnel in UFRGS, Brazil (Blessmann, 1982). The facility has a 100 HP fan in a closed circuit where two types of flow were produced: smooth flow, with a local turbulence intensity of 0.4%, and turbulent flow, with the use of a grid, with a local turbulence intensity of 11%. Sectional models were inserted in the test chamber mid-section ($z_{ref} = 0.45$ m). Vertical profiles indicating the main flow characteristics are plotted in Fig. 3 in terms of longitudinal mean wind